Proton isovector helicity PDF and the twist-3 moment $\tilde{d}_2$ from lattice QCD at physical quark masses

The 43rd International Symposium on Lattice Field Theory (Lattice 2026)

University of Maryland,

College Park, Maryland, USA

July 26 — Aug 1, 2026

YONG ZHAO

X. Gao, H.-T. Shu, **R. Zhang**, et al., Phys. Rev. D 114 (2026), 014505,
X. Gao, **J. He**, J. Lin, et al., arXiv: 2602.11283.

Argonne NATIONAL LABORATORY

Proton spin structure

- Longitudinal spin structure

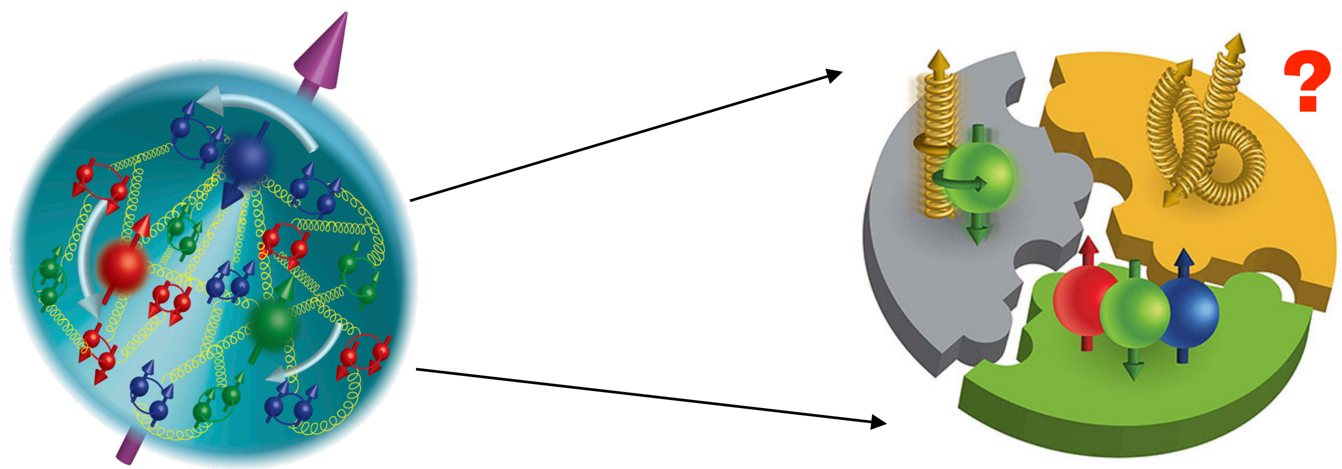

$$= \frac{1}{2} \qquad \Delta\Sigma(Q) = \sum_q \int_{-1}^{1} dx\ g_1^q(x, Q)$$

- Transverse spin structure
  - Structure function: $g_T(x, Q) = g_1(x, Q) + g_2(x, Q)$
  - Genuine twist-3 moment: $\tilde{d}_2(Q) = \int_{-1}^{1} dx\ x^2 \left[3g_T(x, Q) - g_1(x, Q)\right]$

    "Average Lorentz force" on the struck quark.

Status of lattice calculations

- Proton quark helicity PDF:
  - C. Alexandrou et al. (ETMC), PRL **121** (2018), 112001;
  - H.-W. Lin et al. (LP3), PRL **121** (2018), 242003;

    First calculations: isovector, single *a*, physical m_π, P^z_{max}=1.38 GeV (ETMC) and 3 GeV (LP3); LaMET + RI/MOM at NLO.
  - C. Alexandrou et al. (ETMC), PRL **126** (2021), 102003;
  - C. Alexandrou et al. (ETMC), PRD **104** (2021), 054503;

    First flavor separation: single *a*, m_π=260 MeV, P^z_{max}=1.24 GeV; LaMET + RI/MOM at NLO.
  - C. Alexandrou et al. (ETMC), PRD **104** (2021), 054503;

    Isovector, m_π=370 MeV, P^z_{max}=1.9 GeV, continuum limit; LaMET + RI/MOM at NLO.
  - R. Edwards et al. (HadStruc), JHEP **03** (2023) 086;

    Isovector, single *a*, m_π=358 MeV, P^z_{max}=2.5 GeV; Pseudo distribution + double ratio at NLO.
  - J. Holligan and H.-W. Lin, PLB **854** (2024) 138731.

    Isovector, m_π=315 MeV, P^z_{max}=1.7 GeV, continuum limit; LaMET + hybrid LRR +RGR+ NLO.
- $g_T(x)$ and $\tilde{d}_2$ moment:
  - S. Bhattacharya, et al., PRD **102** (2020), 111501;

    First and only $g_T(x)$: isovector, single *a*, m_π=260 MeV, P^z_{max}=1.67 GeV; LaMET + RI/MOM at NLO.
  - M. Gockeler, et al., PRD **72** (2005), 054507;
  - S. Bürger et al., (RQCD), PRD **105** (2022), 054504;
  - J. Crawford et al., (QCDSF), PRL **134** (2025), 071901.

    $\tilde{d}_2$: continuum and/or chiral extrapolation; local operator; nonzero u-d contribution reported by RQCD and QCDSF.

Large-Momentum Effective Theory (LaMET)

$$g_1(x,\mu) = \int_{-\infty}^{\infty} \frac{dy}{|y|} C\left(\frac{x}{y}, \frac{\mu}{2xP^z}, \frac{\tilde{\mu}}{\mu}\right) \tilde{g}_1(y, P^z, \tilde{\mu}) + \mathcal{O}\left(\frac{\Lambda_{\rm QCD}^2}{(xP^z)^2}, \frac{\Lambda_{\rm QCD}^2}{((1-x)P^z)^2}\right)$$

- Power expansion in parton momentum
  - X. Ji, PRL **110** (2013); SCPMA **57** (2014).
  - X. Ji, Y.-S. Liu, Y. Liu, J.-H. Zhang and YZ, RMP **93** (2021).
- Valid for a moderate range of *x* at finite P^z
- No parameterization from global analyses
- Matching kernel available at N³LO now

NNLO
- Chen, Zhu and Wang, PRL. **126** (2021);
- Li, Ma and Qiu, PRL **126** (2021);

N3LO
- Cheng, Huang, Li, Li and Ma, PRL 134 (2025).

- Leading renormalon resummation (LRR) which improves power accuracy
  - Holligan, Ji, Lin, Su and Zhang, NPB **993** (2023);
  - Zhang, Ji, Holligan and Su, PLB **844** (2023).
- DGLAP ($x \to 0$) and threshold ($x \to 1$) resummations (RGR and TR)
  - X. Gao, K. Lee, S. Mukherjee, C. Shugert and YZ, **PRD** 103 (2021);
  - Y. Su, X. Ji, and J. Holligan et al., **NPB** 991 (2023);
  - X. Ji, Y. Liu and Y. Su, **JHEP** 08 (2023) 037;
  - Y. Liu and Y. Su, **JHEP** 2024 (2024) 204;
  - X. Ji, Y. Liu, Y. Su and R. Zhang, **JHEP** 03 (2025).
  - J. Holligan, H.-W. Lin, R. Zhang and YZ, **JHEP** 207 (2025).

Lattice setup

- Nf=2+1 HISQ (HotQCD), physical pion mass
- Wilson-Clover valence fermion, 1 step HYP smeared fields
- Valence $m_\pi \approx 140$ MeV
- $P_z = \frac{2\pi}{L}\{0,1,4,6\} = \{0,0.25,1.02,1.53\}\mathrm{GeV}$
- $t_{\mathrm{sep}}/a = 6,8,10,12$ (12 only for g_A)
- AMA (exact + sloppy solvers), multigrid QUDA, Coulomb-gauge momentum smearing.

β	a [fm]	m_π [GeV]	N_σ	N_τ	# conf.
7.13	0.076	0.14	64	64	350

Highlight: physical point on a fine lattice (a=0.076 fm)

Caveat: largest momentum $P_z = 1.53$ GeV (kinematically enhanced interpolator NOT used)

Workflow (for LaMET):

1. **Bare matrix elements**
2. **Hybrid renormalization + LRR**
3. **Asymptotic extrapolation and Fourier transform (FT)**
4. **Perturbative matching + RGR + TR @ NNLO**
5. **Constraining the end-point regions with short-distance expansion**
6. ~~**Continuum and infinite momentum limits**~~

$\tilde{d}_2$ obtained from the OPE of nonlocal matrix elements.

Bare matrix elements

$$h^{\Gamma}(z, P^z, a) = \langle PS \,|\, \bar{\psi}(z) W(z,0) \Gamma \psi(0) \,|\, \rangle = R = \lim_{t_{\rm sep} \gg \tau \gg a} \frac{C_{\rm 3pt}(t_{\rm sep}, \tau)}{C_{\rm 2pt}(t_{\rm sep})}$$

$$\Gamma = i\gamma_5\gamma_z, i\gamma_5\gamma_x$$

- Isovector channel
- Energy levels from 2-state fits, used as prior for ratio analyses
- Omit 2 times slices in τ near the source-sink to suppress excited-state contamination
- Uncorrelated fits with bootstrap resampling.

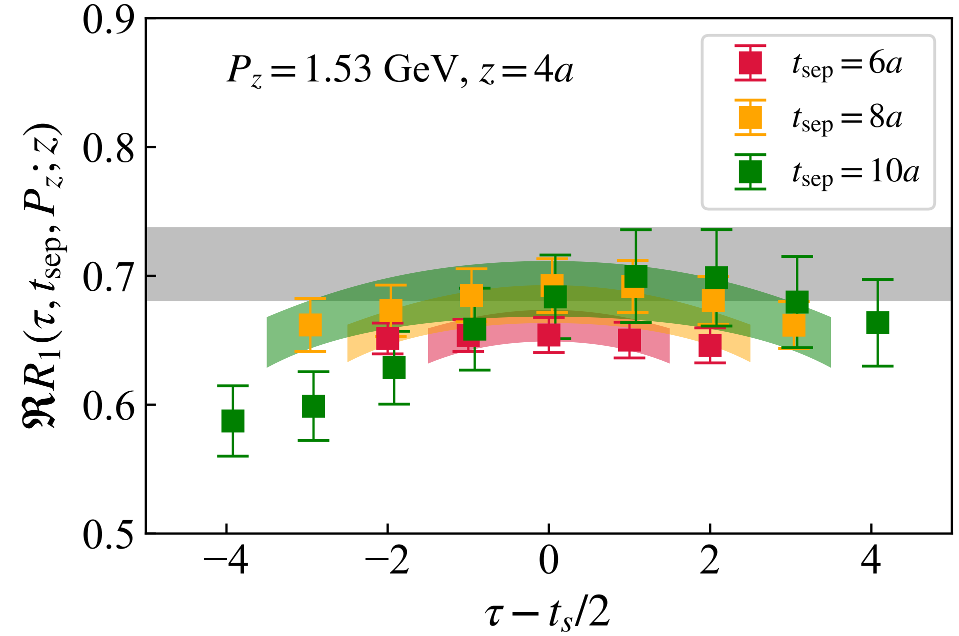

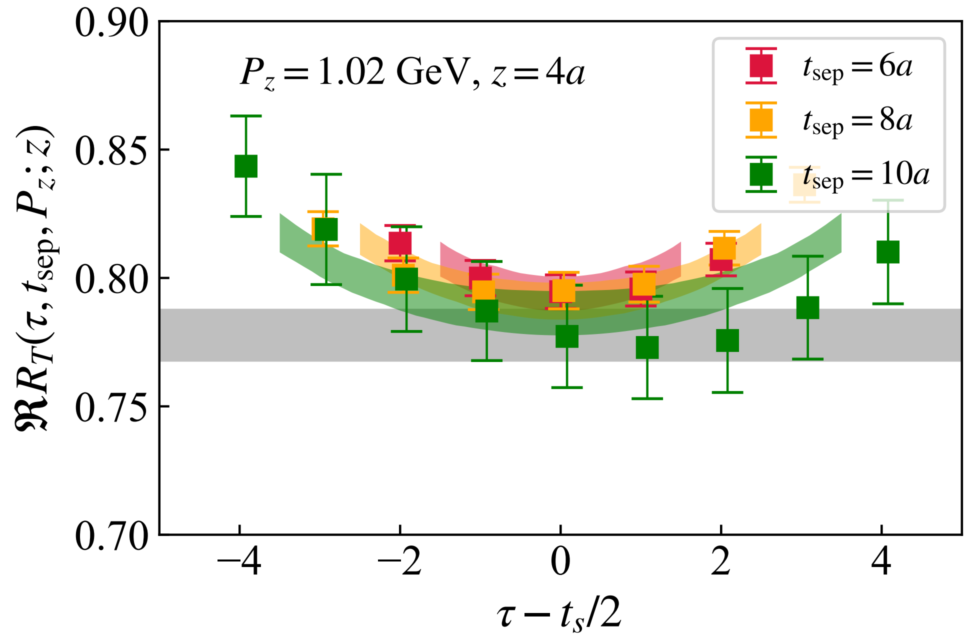

Bare matrix elements

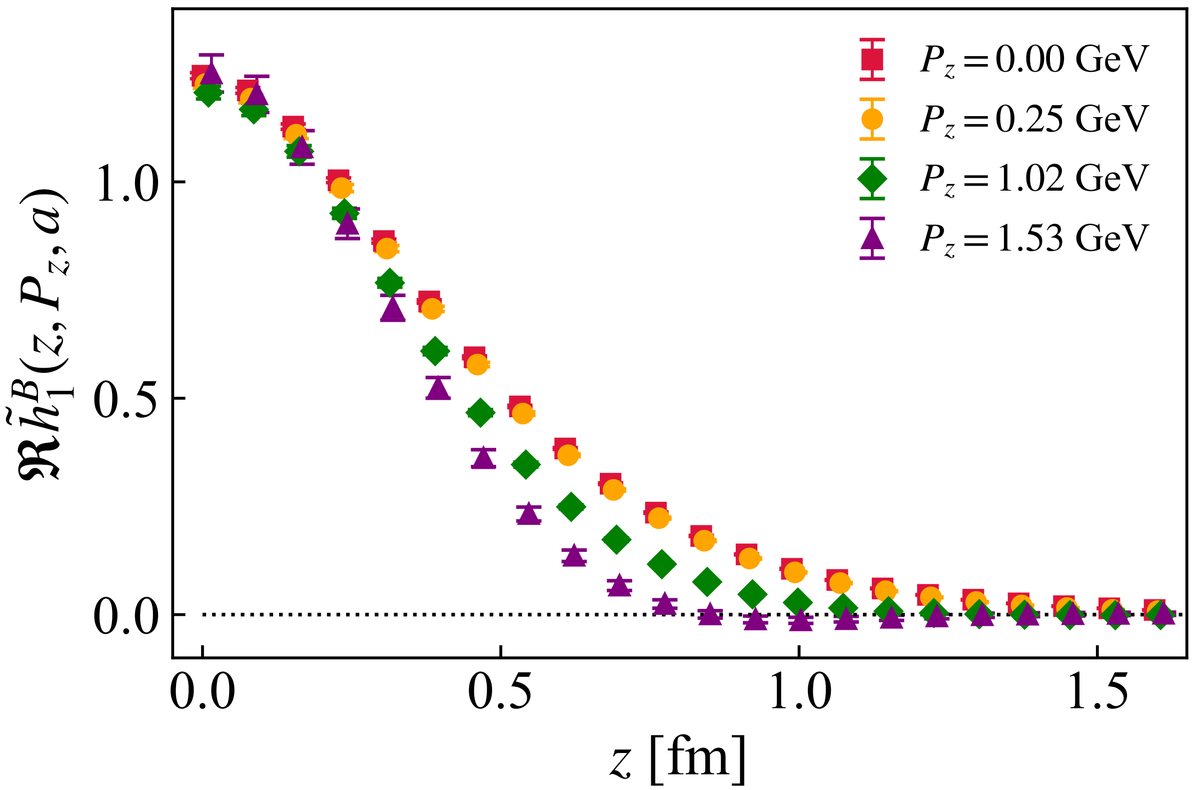

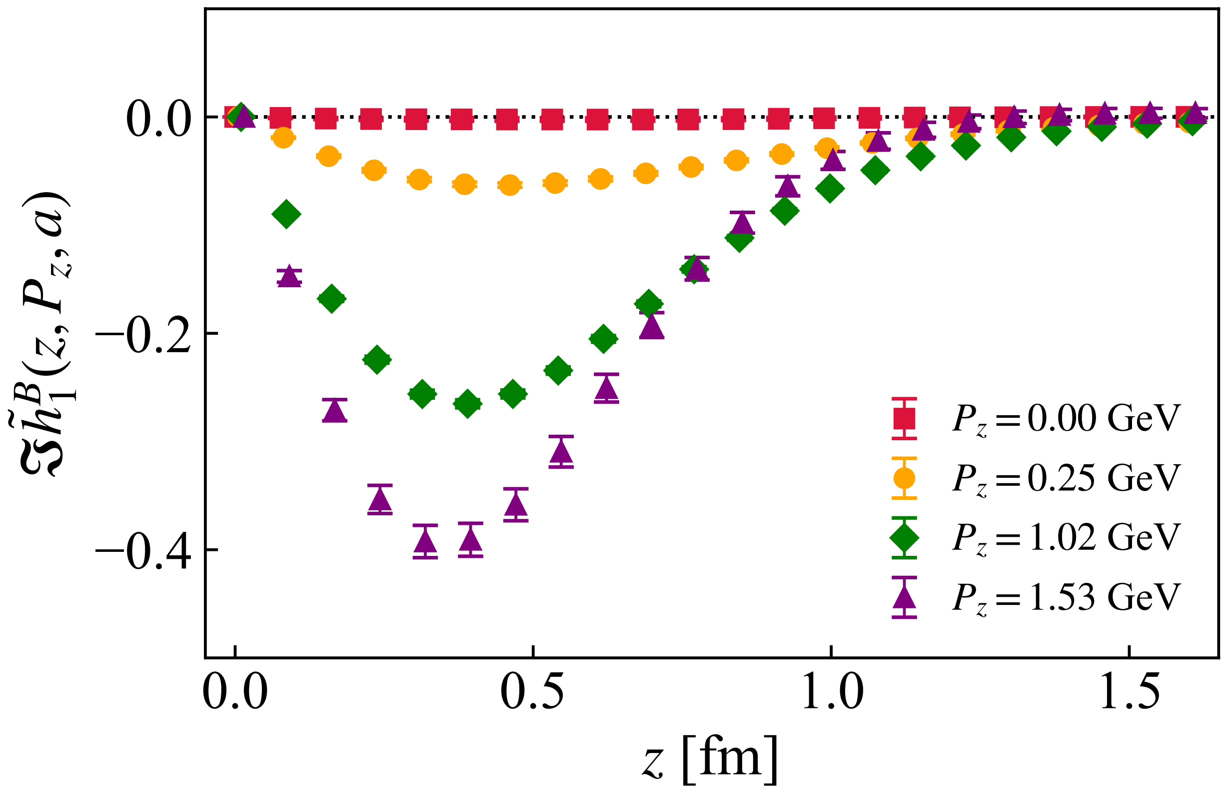

At *z=0*, the local matrix elements agree, $g_A = Z_A \tilde{h}_1(0)$

Axial charge $g_A = 1.211(12)$

Hybrid renormalization

$$\tilde{h}_1^R(z, P_z) = \begin{cases} \frac{\tilde{h}_1^B(z,P_z,a)}{\tilde{h}_1^B(z,0,a)} & |z| \le z_s \\ \frac{\tilde{h}_1^B(z,P_z,a)}{\tilde{h}_1^B(z_s,0,a)} e^{(\delta m + m_0)(z-z_s)} & |z| \ge z_s \end{cases}$$

- $a\delta m(a) = 0.1597(16)$ from the static potential
- Renormalon ambiguity in $\delta m(a)$ removed by $m_0(\tau) \sim \Lambda_{\rm QCD}$, which is fitted from the short-distance $P^z = 0$ matrix elements with LRR Wilson coefficient $C_0(z^2\mu^2)$

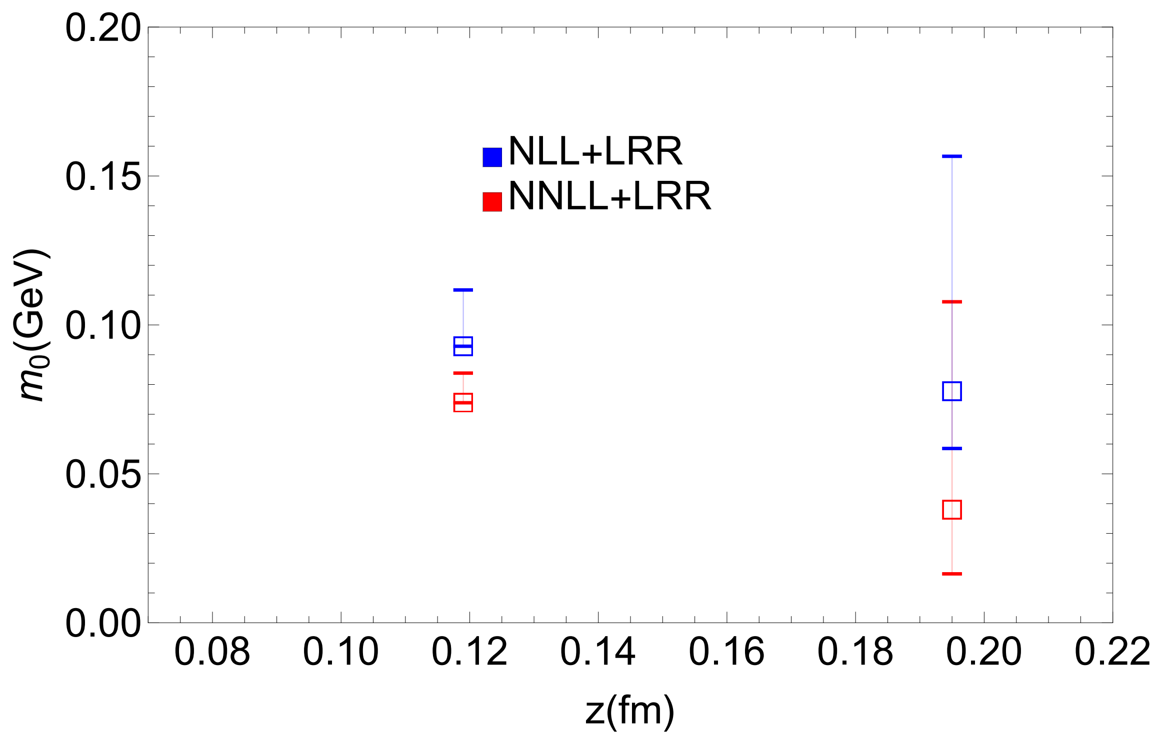

$m_0(\tau) \lesssim 0.1$ GeV

Asymptotic extrapolation & FT

- Complete the FT using smoothness & asymptotic behavior of correlation functions: essentially the same requirements for numerical integrations.
- Is the asymptotic region reached yet? The bare matrix elements can tell.
- Can be combined with methods to estimate the other systematics, such as excited-state contamination.

  - Target form (form 2), rigorously derived from dispersion relation
    - Ji, Liu, Su, arXiv: 2601.12189.

$$\lim_{|z|\to\infty} \tilde{h}_1(z, P^z) = \left[A(P^z)e^{i\phi \mathrm{sgn}(z)} + \frac{A'(P^z)e^{i\phi' \mathrm{sgn}(z)}}{|z|} \right] e^{-\Lambda |z|}$$

$$\Lambda \approx 0.47(11)\ \mathrm{GeV}\,, \chi^2/\mathrm{dof} = 0.78$$

  - Reference form (form 1), used in earlier analyses

$$\frac{Ae^{-m_{\mathrm{eff}}|z|}}{|zP^z|^d}$$

- Ji, Liu, Schäfer, et al., NPB 964 (2021) 115311;
- X. Gao, YZ et al., PRL 128 (2002), 142003.

$$m_{\mathrm{eff}} \approx 0.77(60)\ \mathrm{GeV}\,, \chi^2/\mathrm{dof} = 1.47$$

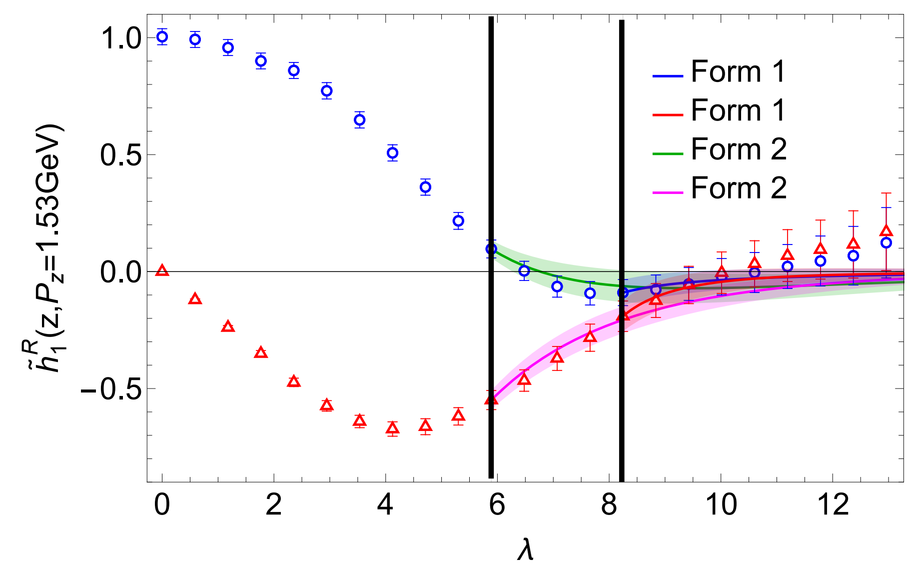

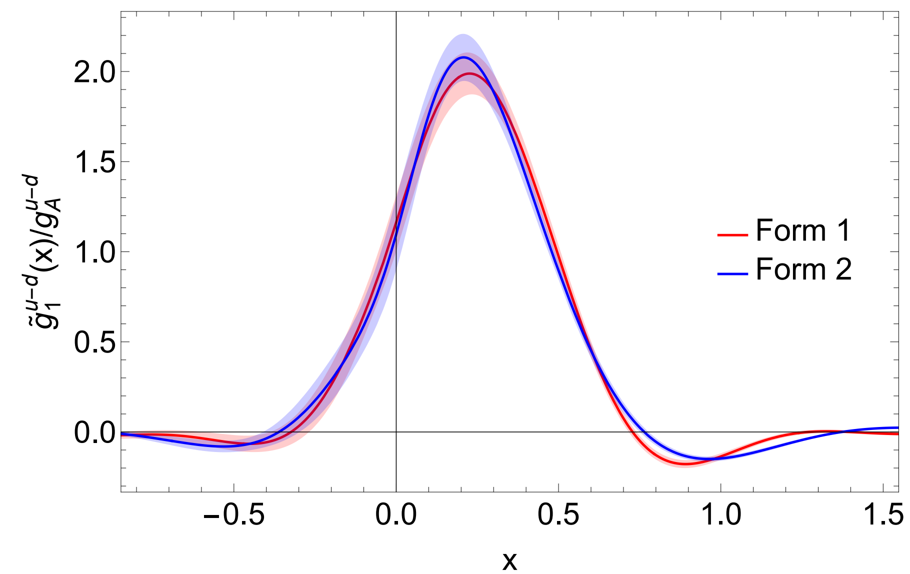

Perturbative matching with resummations

RGR+TR+LRR at NNLO:

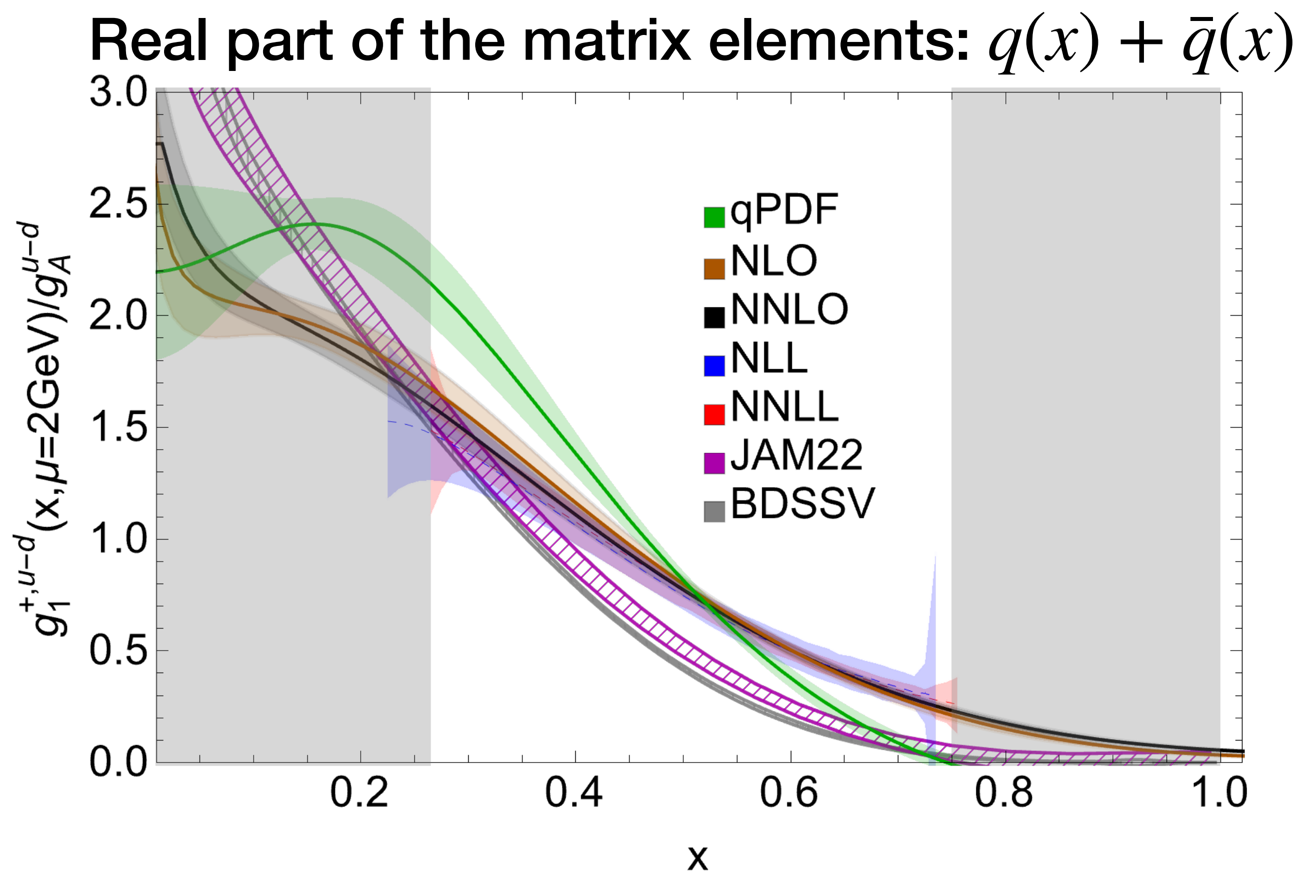

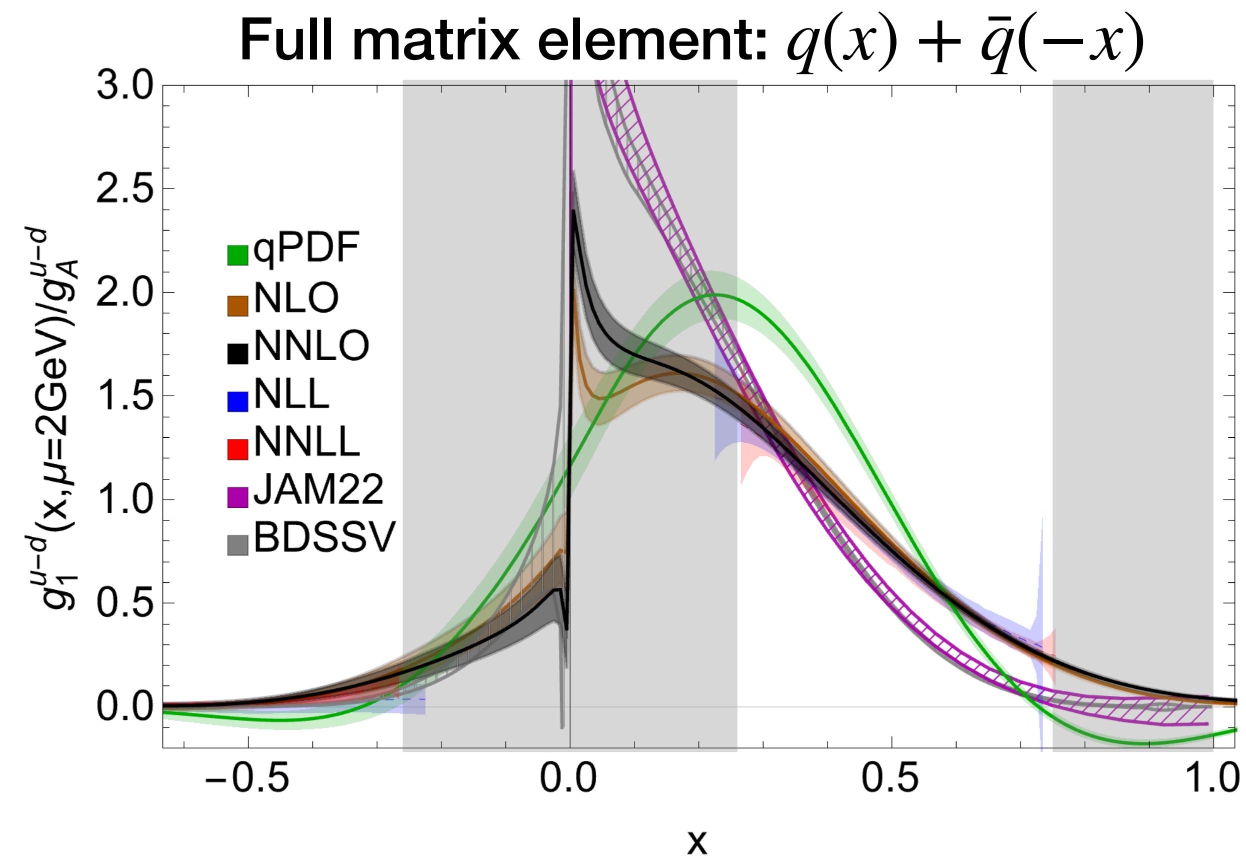

After resummations, the window for perturbation theory to converge is $[x_0, 1 - x_0]$ with $x_0 \sim \Lambda_{\mathrm{QCD}}/(2P^z)$. Here $x_0 \approx 0.25$ by requiring scale variation uncertainty ($\kappa \in [1/\sqrt{2}, \sqrt{2}]$ in $\mu_0 = 2\kappa x P^z$) to remain finite.

Results from the Coulomb-gauge method

- HotQCD ensemble, $a = 0.06$ fm, $V_s \times T = 48^3 \times 64$, $m_\pi = 300$ MeV, $P^z = \{2.43,\ 3.04\}$ GeV, Hybrid scheme + RGR + NLO.

- Caveat: did not normalize the matrix elements by $\tilde{h}_1(0,P^z,a)/\tilde{h}_1(0,0,a)$.

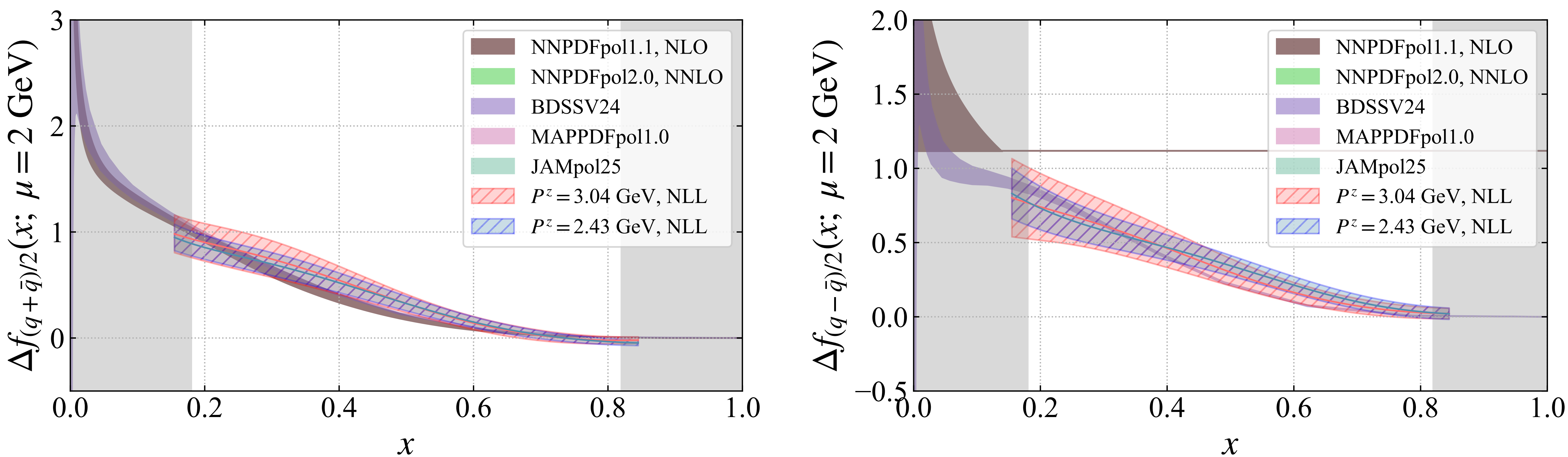

X. Gao, J. He, J. Lin, et al., arXiv: 2602.11283.

Comparison with the Coulomb-gauge results

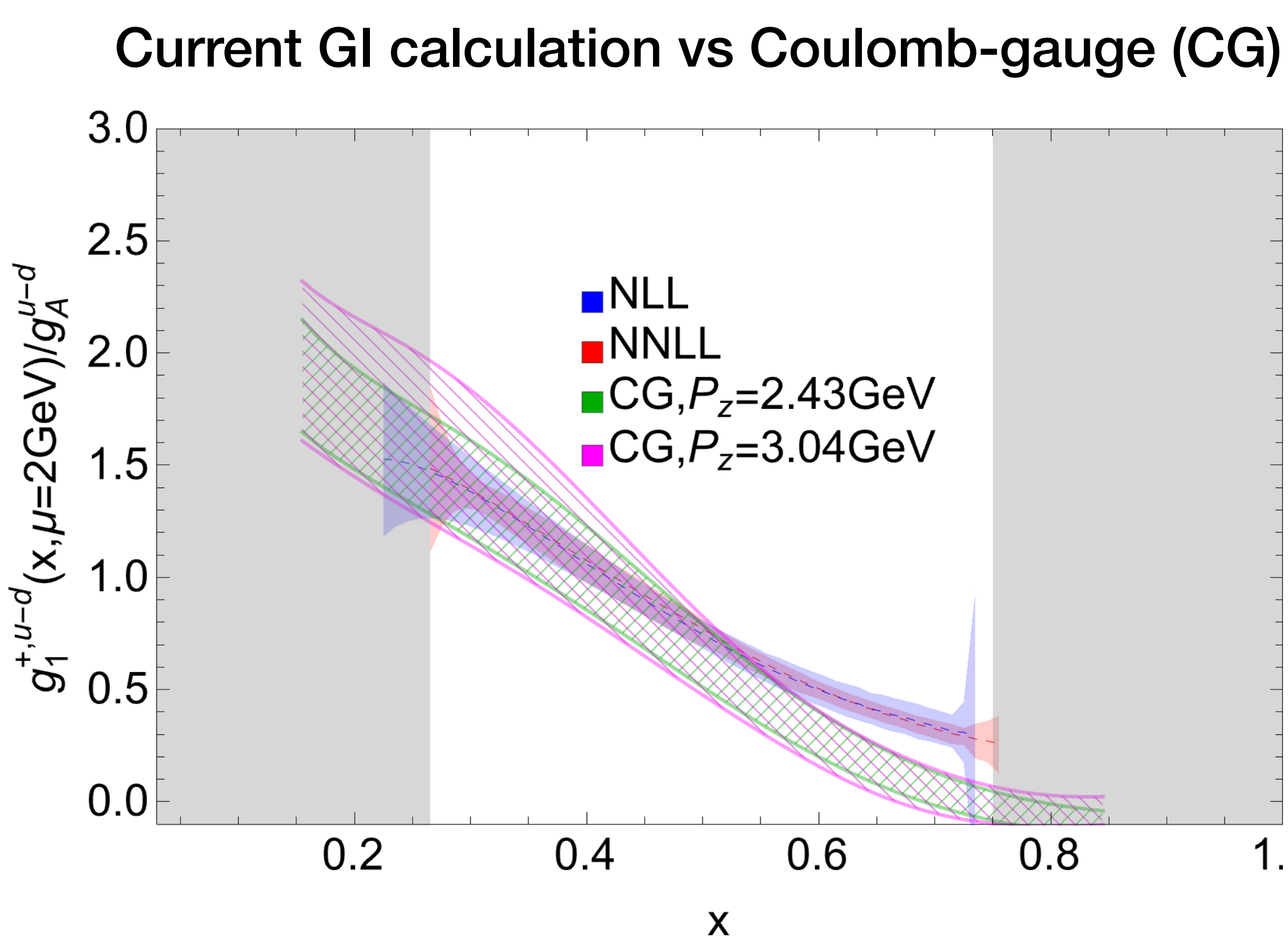

Calculations at higher momenta tend to be closer to the global analyses at x>0.5.

Complementarity

- Model end-point regions:

- X. Ji, Research 8 (2025) 0695.

$$g_1(x) = \begin{cases} f(x_0)\frac{x^a}{x_0^a}, & x < x_0 \\ f(x), & x_0 < x < 1 - x_0 \\ f(1-x_0)\frac{(1-x)^b}{(1-x_0)^b}, & x > 1 - x_0 \end{cases}$$

- Fit parameters *a, b* from short-distance matrix elements.
    - Fit double ratio at z={1,2,3}a;
    - $x_0 = 0.3$;
    - $g_1^{q+\bar{q}}$: a=-0.38(9), b=1.68(87), $\chi^2/\mathrm{dof} = 0.16$
    - $g_1^{q-\bar{q}}$: a=-0.10(83), b=0.15(22), $\chi^2/\mathrm{dof} = 1.21$

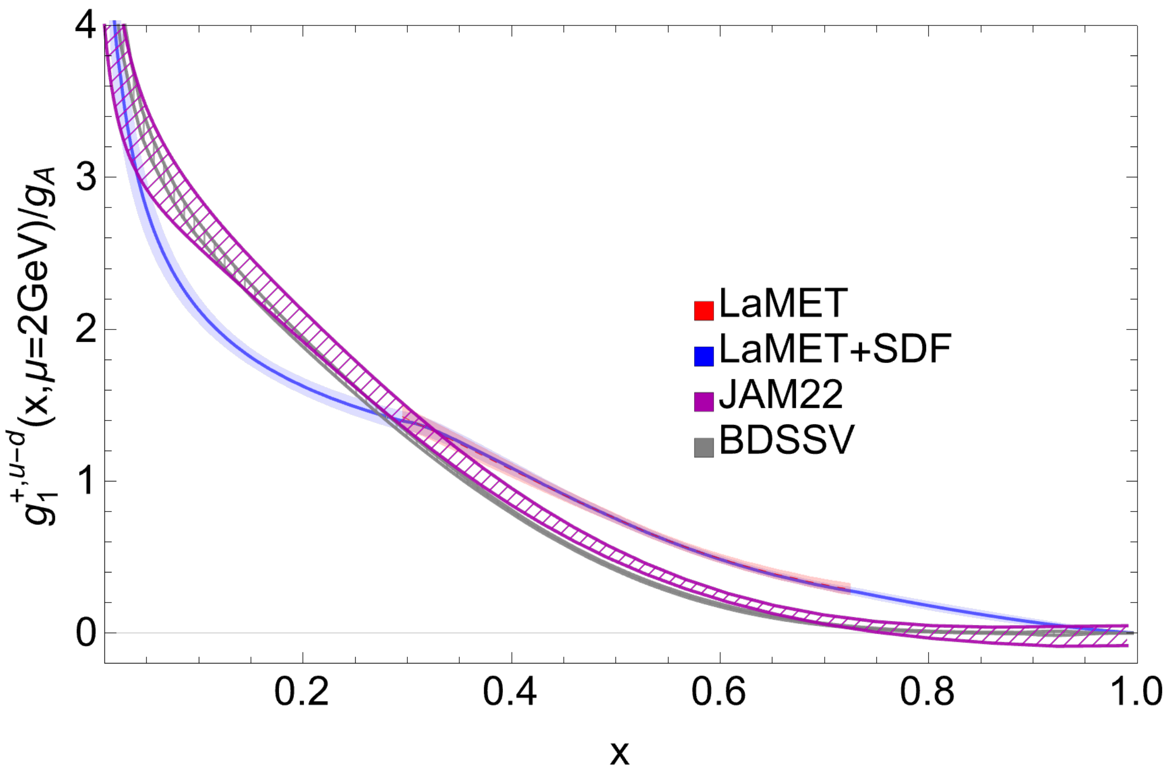

Operator product expansion

- RG-invariant double ratio:

K. Orginos, A. Radyushkin, J. Karpie, S. Zafeiropoulos, PRD 96 (2017), 094503

$$\mathcal{M}_T(\lambda, z^2) \equiv \frac{\tilde{h}_T^B(z, P_z)}{\tilde{h}_T^B(z, 0)} \frac{\tilde{h}_T^B(0, 0)}{\tilde{h}_T^B(0, P_z)} = \frac{\tilde{h}_T^{\overline{\mathrm{MS}}}(\lambda, z^2\mu^2)}{\tilde{h}_T^{\overline{\mathrm{MS}}}(0, z^2\mu^2)}.$$

- OPE at NLO:

Wandzura-Wilczek approximation

$$\mathcal{M}_T^{\mathrm{tw3}}(\lambda, z^2\mu^2) \equiv \mathcal{M}_T(\lambda, z^2\mu^2) - \frac{\tilde{h}_1^{\overline{\mathrm{MS}}}(0, z^2\mu^2)}{\tilde{h}_T^{\overline{\mathrm{MS}}}(0, z^2\mu^2)} \int_0^1 d\alpha\, \mathcal{M}_1(\alpha\lambda, z^2\mu^2) - \frac{1}{\tilde{h}_T^{\overline{\mathrm{MS}}}(0, z^2\mu^2)} \left(-\frac{\alpha_s C_F}{\pi} a_0 + i\,\lambda\, \frac{\alpha_s C_F}{3\pi}\, a_1\right)$$

$$= \frac{\lambda^2}{3} \frac{\left\{\tilde{d}_2 + \frac{7\alpha_s C_F}{24\pi}\, a_2 + \frac{\alpha_s}{4\pi}\tilde{d}_2 \left[\left(\frac{43C_F}{12} + \frac{9}{4N_c} + \frac{3N_c}{4}\right) L_z - \frac{13C_F}{4} + \frac{3}{4N_c} - \frac{3N_c}{4}\right]\right\}}{C_0(z^2\mu^2)a_0 - \frac{\alpha_s C_F}{\pi}\, a_0} + \mathcal{O}(\lambda^3)$$

- a_0, a_1, a_2 are moments of the helicity PDF;

V. Braun, Y. Ji, A. Vladimirov, JHEP 05 (2021), 086

- RGR not included for this exploratory calculation.

The $\tilde{d}_2$ moment

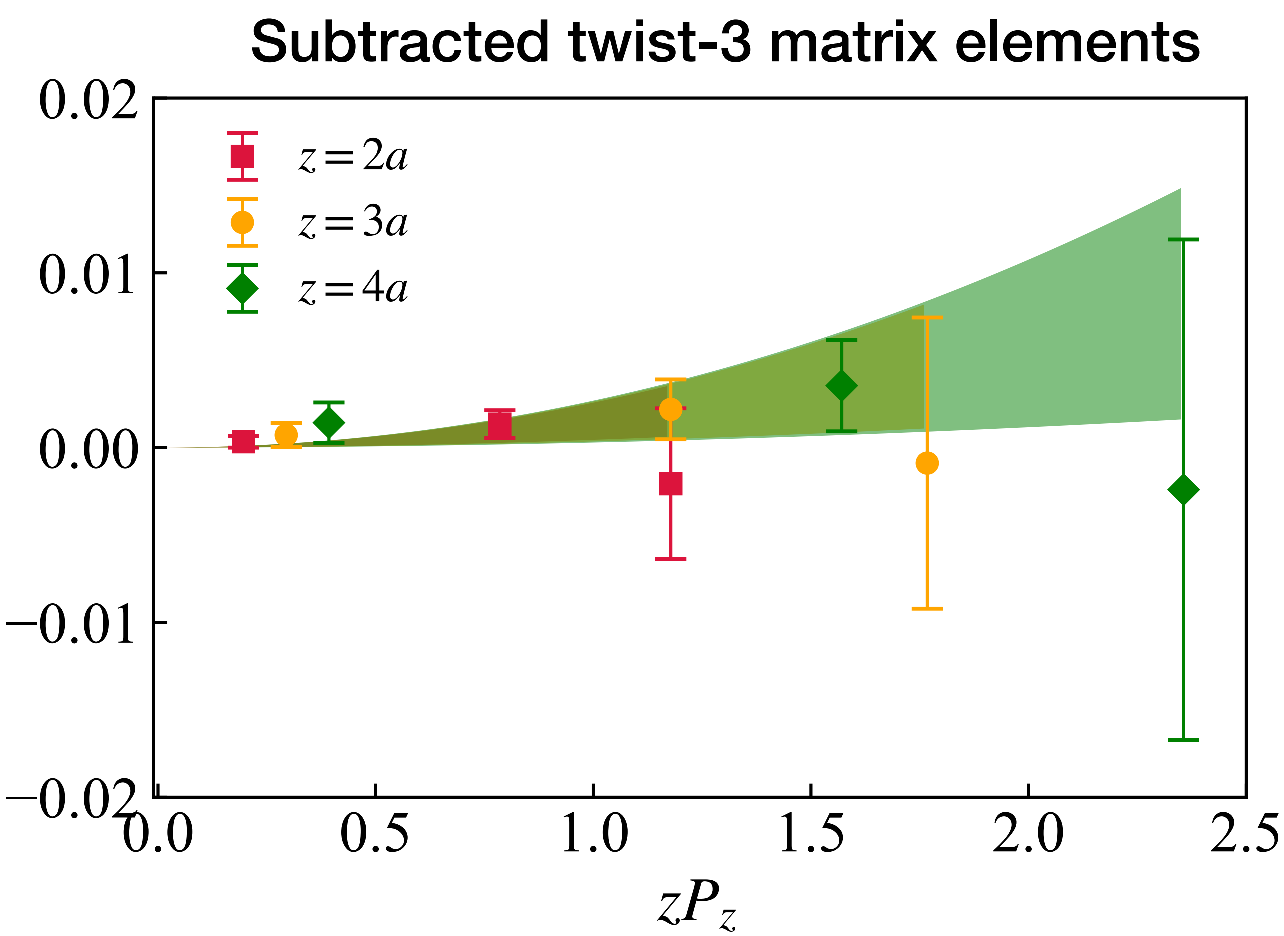

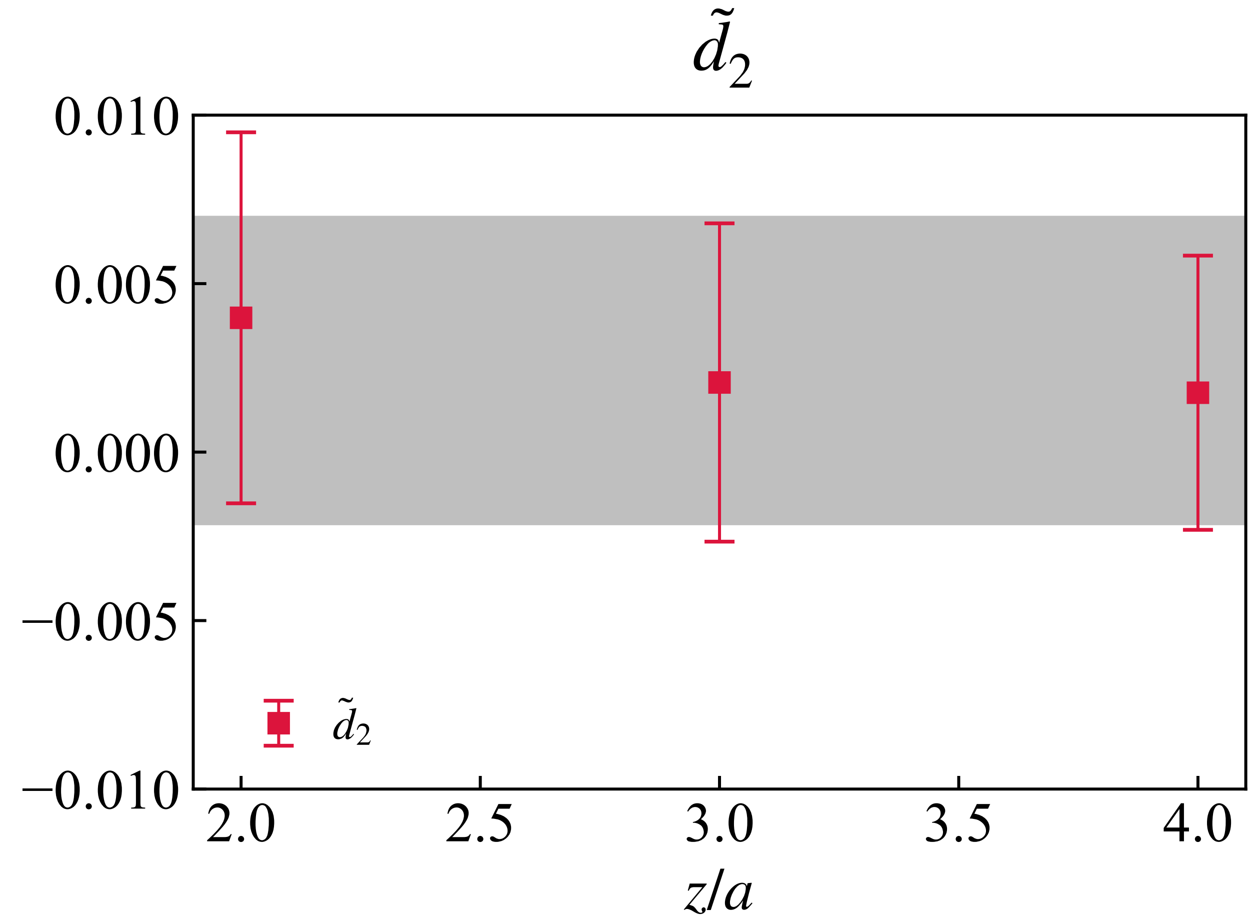

$$\tilde{d}_2^{u-d}(\mu = 2\ \mathrm{GeV}) = 0.0024(46)$$

Gockeler, et al (2005): 0.002(2)

RQCD (2022): 0.0038(33)

QCDSF (2025): 0.008(3)(2)

Moments of the helicity PDF

- OPE at NNLL with RGR.

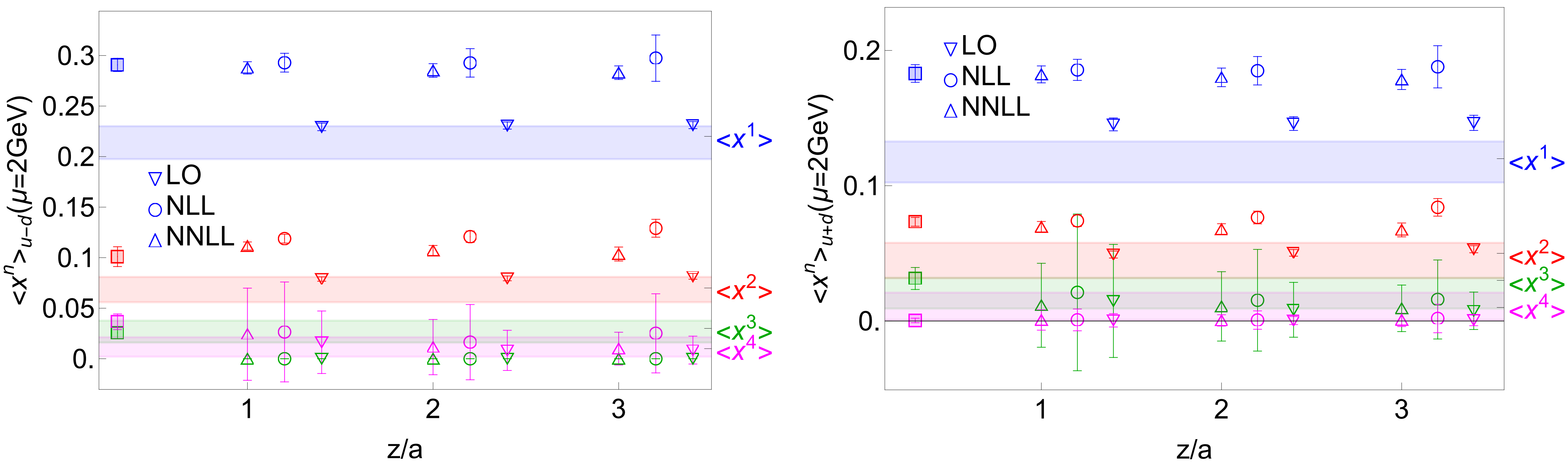

Both <x> and <x^2> are higher than those from JAM22 (bands), which corresponds to the deviation at moderate x in momentum space.

Summary

- The proton isovector helicity PDF has been calculated with up-to-date LaMET analysis at physical quark masses and momentum P^z=1.53 GeV;
- The GI approach shows consistency with the CG approach at moderate x, while the CG results at larger P^z tend to have better agreement with global analyses.
- We also extracted the twist-three moment $\tilde{d}_2$, which is consistent with zero.
- More work need to be done in the future to quantify the power correction, discretization artifacts, and also reduce the excited-state contamination. Note the lesson from the calculation of g_A.